I&EC research
Industrial & Engineering Chemistry Research

Article

pubs.acs.org/IECR

Polystyrene Foaming at High Pressure Drop Rates

Daniele Tammaro,[†] Antonello Astarita,[†] Ernesto Di Maio,*[,†] and Salvatore Iannace[‡]

[†]Dipartimento di Ingegneria Chimica, dei Materiali e della Produzione Industriale, Università degli Studi di Napoli Federico II, Piazzale Tecchio 80, I-80125 Napoli, Italy

[‡]Istituto per lo Studio delle Macromolecole, Consiglio Nazionale delle Ricerche, Via E. Bassini 15, I-20133 Milano, Italy

ABSTRACT: We studied the foaming of polystyrene with CO_2 as the physical blowing agent at large pressure drop rates (PDRs) and at different foaming temperatures, with a novel batch foaming apparatus, capable of reaching PDRs as high as 500 MPa/s (in the underlying literature, the maximum so far achieved is 100 MPa/s). Results show that, at each foaming temperature, the number of nucleated bubbles per unit initial volume (N) linearly increases with PDR in a bilogarithmic scale, with slopes increasing with the temperature. The effect of talc as the nucleating agent was also investigated. Furthermore, a phenomenological model was developed and utilized to predict N at PDRs not experimentally accessible. The approach was validated and a good agreement with the experimental data was obtained.

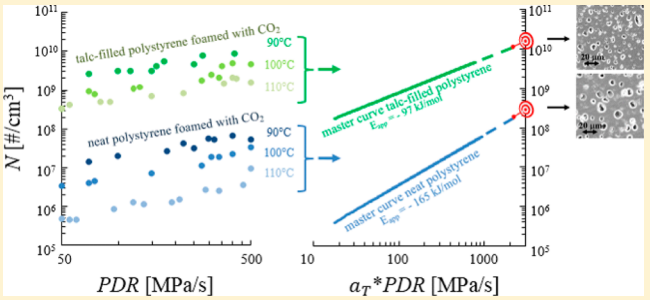

INTRODUCTION

In thermoplastic foaming with a physical blowing agent, the pressure drop rate, PDR (i.e., the rate at which the saturation pressure is reduced to ambient pressure by the blowing agent release), is an important processing variable,[1] being involved in the competition between the bubble nucleation and growth.[2,3] Many authors investigated the effect of PDR on the foam morphology and, to do so, designed foaming apparatuses capable of achieving, in similar foaming conditions, different PDRs. For instance, Guo et al.[4] designed a batch foaming system to "online" visualize the nucleation phenomenon at high PDR. Their system was used with polystyrene (PS)/CO_2, and the results showed that a higher number of nucleated bubbles are observed with increasing PDRs. From a modeling point of view, Taki[5] developed a model of bubble nucleation and growth to predict the number of nucleated bubbles per unit initial volume (N) as a function of the PDR and validated it with a polypropylene (PP)/CO_2 system. Tsivintzelis et al.[6] reported foam morphologies of PS/CO_2 obtained at different PDRs, observing that the mean pore diameter decreased and N increased with an increase of the PDR. In fact, as a general understanding, the increase of the PDR increases the rate of stable nuclei formation, meanwhile reducing the chances for the blowing agent to inflate the newly formed bubbles, with a corresponding refinement of the cellular structure.[4] Classical nucleation theory can be invoked, in this context.[7] The thermodynamic instability induced by the pressure drop nucleates, in the polymer matrix, a myriad of bubbles that then grow because of diffusion of excess gas into the bubble. The nucleation and growth process, during the foaming time, competes to avail the excess gas in the system, and if the PDR is increased, the nucleation is favored and a greater number of cells are formed.

In this context, a very interesting question naturally arises: what happens if the PDR is further increased? Is there a limit to the increase of N with the PDR? Khan et al.[8] investigated the effect of the PDR on the cell size and N on poly(methyl methacrylate) and developed a validated model in a large range of PDRs. They experimentally confirmed the increase of N with the PDR. In addition, they reached a certain critical PDR above which N attains a constant threshold. Other investigators, on other polymer/gas systems, did not find any threshold at high PDRs. More recent works[23,24] modeled the effect of the PDR on bubble nucleation and derived a dimensionless parameter depending on the critical radius (as defined in the framework of classical nucleation theory), on the polymer/blowing agent diffusivity, and on the PDR, to describe the PDR limit above which N reaches a threshold. In their case, the threshold corresponded to ca. 10 GPa/s, as extrapolated from data in refs 4−6. Nevertheless, it is reasonable that the presence of a PDR above which N reaches a threshold depends on the polymer/gas system. It is also clear that the way N changes at high PDR and the possible presence of a threshold are both not well understood and are both interesting open problems. In fact, conventional vessels for polymer foaming do not reach very high PDRs. In this context, some of the authors developed a batch foaming equipment, called "minibatch", to substantially increase PDRs with respect to conventional vessels.[9] In the present paper, we utilized the minibatch to investigate the morphology of PS foams blown with CO_2 on a wide range of PDRs (i.e., from 50 to 500 MPa/s). Furthermore, we studied

Received: December 23, 2015
Revised: March 2, 2016
Accepted: April 13, 2016

DOI: 10.1021/acs.iecr.5b04911
Ind. Eng. Chem. Res. XXXX, XXX, XXX−XXX

how the effect of talc as a nucleating agent influences bubble nucleation, at different PDRs and foaming temperatures (T_{foam}). To describe the gathered results, a modified version of a model by Muratani et al. was used.[10] This approach allows one to predict N at different T_{foam} and PDR values, with or without talc. Validation of the approach was conducted, and a good agreement between the model prediction and experimental data was obtained.

MATERIALS AND METHODS

Polystyrene (PS; N2380) was supplied by Versalis SpA (Mantova, Italy) and used as received. The average molecular weight, density, and melt flow index are 300 kDa, 1.05 g/cm^3, and 2.0 g/10 min at 200 °C and 10 kg, respectively, as reported by the producer. Talc, supplied by Imerys Talc (Toulouse, France) with a median particle size equal to 1.8 μm, was used as the nucleating agent in 1 wt % mixtures. The constituents (i.e., PS and talc), dried overnight under vacuum at 90 °C, were melt-compounded in a corotating twin-screw extruder (15 mL Micro Compounder, DSM Xplore, Geleen, The Netherlands). The extrusions were performed at 210 °C in a nitrogen atmosphere. The screw speed was 150 rpm, corresponding to average shear rates of ca. 75 s^{-1}, and the residence time, accurately controlled by means of a backflow channel, was 240 s. The extrudate was granulated for subsequent foaming experiments. After the mixing procedure, a homogeneous dispersion of talc particles in the polymer matrix was confirmed by scanning electron microscopy (SEM) analysis (data not reported). CO_2 (99.95% pure), supplied by Sol Group SpA (Monza, Italy), was used as the physical blowing agent.

The foaming apparatus utilized in this study, the minibatch, was designed by Tammaro et al.[9] to maximize the PDR by minimizing the volume to be evacuated, which allowed one to reach PDRs as high as 500 MPa/s from a saturation pressure of 10 MPa and up to 1800 MPa/s from a saturation pressure of 30 MPa. Control of the processing parameters was achieved by means of a PID controller (model X1, Ascon-New England Temperature Solutions, Attleboro, MA) and a syringe pump 500D (Teledyne Isco, Lincoln, NE). A pressure transducer (model P943, Schaevitz-Measurements Specialties, Hampton, VA) was used to measure the pressure, and the pressure history was registered using a data acquisition system (DAQ PCI6036E, National Instruments, Austin, TX). The pressure release system consisted of a discharge valve (model 10-80NFH, High Pressure Equipment Company, Erie, PA) and a pneumatic electrovalve. The pressure discharge system was designed to allow many different PDRs, from the same P_{sat}, by using different ball valves actuating pressure and/or different downstream piping. There is an ongoing debate in the literature on the proper way to describe the shape of the pressure versus time curve.[4,8] In order to compare the results achieved with different pressure histories and with different apparatuses, the absolute maximum PDR is, in our point of view, the most suitable description, and PDRs, associated with the different pressure versus time curves, were calculated as the highest mean value of the derivative of the pressure history over a period of 0.010 s, using a data acquisition frequency of 1000 Hz.

In a typical experiment, two polymer cylinders, with an average characteristic size of 1.5 ± 0.1 mm (one of neat PS and one of PS filled with 1 wt % talc particles), were placed in the minibatch. After sample loading, the vessel was heated to the saturation temperature (T_{sat}) and the pressure was increased up to a saturation pressure (P_{sat}) of 10 MPa. After a solubilization time of 4 h,[11] during which P_{sat} and T_{sat} were maintained constant, the pressure was quenched to ambient pressure. In this procedure, in the different tests, T_{sat} was always equal to T_{foam}.

The foams were characterized to determine their densities (ρ) and N. ρ was measured according to ASTM D792, using an analytical balance (Mettler Toledo, Columbus, OH). The cellular structure of the foams was investigated by using a scanning electron microscope. The samples were first sectioned with a razor blade in liquid nitrogen and then coated with gold using a sputter coater. N was calculated as $N = \left(\frac{n}{A}\right)^{3/2}\left(\frac{\rho_p}{\rho}\right)$, where n is the number of the cells in the area A of the SEM micrograph and ρ_p is the density of the solid sample.

As described by Tammaro et al.,[9] two kinds of foamed samples may be generated with the minibatch: (1) retained samples, which are foamed within the vessel and subsequently removed after opening the vessel, and (2) expelled samples, which are dragged out by the escaping gas toward the exit of the vessel for a fast extraction and cooling. In the current work, we will only consider retained samples.

A further advantage of the minibatch apparatus, and, in particular, of the minimization approach, is the very accurate measurement of the local temperature and pressure experienced by the sample and the virtual absence of any spatial temperature or pressure gradients within the sample itself. Foaming of larger samples, in industrial practice or when larger pressure vessels are used, may induce the occurrence of PDR or temperature spatial gradients, which, in turn, affects the nucleation and growth phenomena. In the case of larger samples, a comparison with our results and/or adoption of the proposed time−temperature superposition should be done with greater care to address the possible local changes in the processing conditions.

RESULTS

Three sets of experiments were performed at three different T_{foam} values (i.e., 90, 100, and 110 °C), with PDRs ranging from 50 to 500 MPa/s, for samples with and without talc. The results are reported in Figures 1−5.

Figure 1 shows the effect of the PDR on N at all of the investigated T_{foam} values for neat PS. It is evident that N

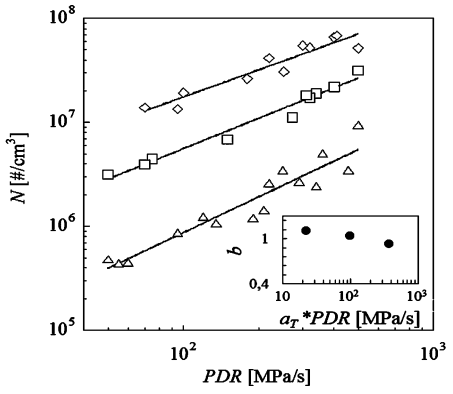

Figure 1. N of neat PS foams as a function of the PDR and at different T_{foam} values (◇, 90 °C; □, 100 °C; △, 110 °C). The solid lines are obtained by interpolation with $N = a\text{PDR}^b$ (see the text for details). The inset shows b as a function of a_TPDR.

DOI: 10.1021/acs.iecr.5b04911
Ind. Eng. Chem. Res. XXXX, XXX, XXX−XXX

increases with the PDR, in the entire investigated range of PDRs, as was expected and described in the introductory part. In fact, linear behavior on a log−log scale is observed, indicating an exponential dependence ($N = a\text{PDR}^b$). For instance, Taki[5] reported a similar behavior of N with PDRs (from 0.001 to 1 MPa/s) in a bilogarithmic scale for PP foamed with CO_2 at 200 °C and 11 MPa. In the current study, the linear dependence is confirmed on the PS/CO_2 system at high PDRs (i.e., 50−500 MPa/s) and at three different T_{foam} values. The slopes b [in (#/cm^3)(s/MPa)], of the interpolating lines for N versus PDR data, increase with T_{foam}. In particular, b is equal to 0.92 at 90 °C, 1.03 at 100 °C, and 1.10 at 110 °C. In the Figure 1, the inset shows b as a function of the PDR in a logarithmic scale. Concerning the relationship between N and T_{foam}, at constant PDR, for this specific case of CO_2-foamed PS, in the processing range explored in this contribution, N decreases with T_{foam}. A theoretical consideration can be invoked to explain the decrease of N with T_{foam}. In particular, the solubilized gas from 90 to 110 °C decreases by about 10%, and this, of course, affects both the nucleation and growth. It is well-known that the rate of the nucleation varies exponentially with the concentration of the solubilized gas;[7] in the meantime, some polymer properties are changing with the concentration of the solubilized gas as well.[11,15,18,26] In the underlying literature, the effect of T_{foam} on N has been extensively studied. Both an increase and a decrease of N with T_{foam} have been observed,[16,24,25] with the discussions relying on the concurrent effects of the temperature on the properties of the specific polymer/blowing agent system of interest in foaming (e.g., polymer viscosity, mutual diffusivity, interfacial tension, and specific volume).[11,26] In our case, we addressed this 1 order of magnitude increase of N, as the temperature decreases from 110 to 90 °C, to the increases of the solubilized CO_2.

Figure 2 shows the effect of the PDR on ρ of neat PS foams, in the PDR interval ranging from 50 up to 500 MPa/s. It is

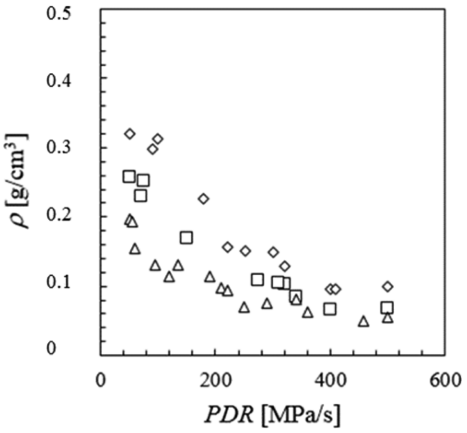

Figure 2. ρ of neat PS foams as a function of the PDR and at different T_{foam} values (◇, 90 °C; □, 100 °C; △, 110 °C).

evident that ρ first decreases with the PDR, and then it reaches a plateau value for the PDR higher than ca. 300 MPa/s. Considering one single temperature, all of the samples were subjected to the same saturation conditions (P_{sat} is the same for all of the samples; see the section on the foaming procedure), which correspond to the same equilibrium concentration of the blowing agent.

In order to explain the effect of the PDR on ρ, the following hold true: (i) nucleation is faster, with an increase of the PDR (the thermodynamic instability responsible for the bubble formation is reached earlier);[25] (ii) with an increase of the nucleation, growth is faster because the diffusive path to reach a bubble is shorter while (iii) the effect of the gas concentration on diffusion is minor, typically.[26] Hence, we may observe that, at higher PDR, the whole foaming process is faster and gas loss, in the surroundings from the free surface of the sample, is minimized because it solely depends on the exposure time, with a corresponding increased efficiency in the use of the blowing agent. We may speculate, in these foaming conditions, that, at PDRs of ca. 300 MPa/s and higher, the gas loss from the free surface is negligible and the minimum ρ, for the specific polymer/gas mixtures foamed at a specific T_{foam}, is achieved.

Considering one single PDR, the results show a decrease of ρ with an increase of T_{foam}, due to the favored growth of the bubbles in a less viscous medium, as was also shown by Arora et al.[13] Finally, in this range of processing conditions, the minimum achievable density is 0.06 g/cm^3.

Figure 3 shows the effect of the PDR on N at all of the T_{foam} values for talc-filled PS. It is well-known that talc particles

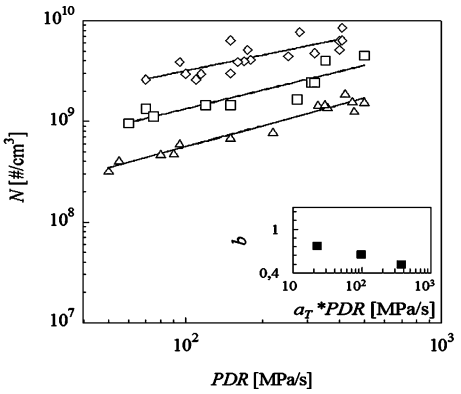

Figure 3. N of talc-filled PS as a function of the PDR and at different T_{foam} values (◇, 90 °C; □, 100 °C; △, 110 °C). The solid lines are obtained by interpolation with $N = a\text{PDR}^b$ (see the text for details). The inset shows b as a function of a_TPDR.

induce heterogeneous nucleation,[19−21] and this explains the larger N (by ca. 3 orders of magnitude) with respect to the neat PS, reported in Figure 1. Furthermore, N linearly increases with the PDR for talc-filled PS, in a bilogarithmic scale also as observed for neat PS. For talc-filled PS, however, the effect of T_{foam} and PDRs on N is smaller than that for neat PS (the slopes of the interpolating lines at the different T_{foam} values are smaller than those calculated for neat PS). In effect, for talc-filled PS at T_{foam} equal to 110, 100, and 90 °C, the slopes are respectively equal to 0.76, 0.64, and 0.51 [in (#/cm^3)(s/MPa)]. In addition, a 10-fold increase of N is observed when T_{foam} increases from 90 to 110 °C, while in the case of neat PS, a 15-fold increase has been observed. The decreased dependence of N with T_{foam} in the case of talc-filled PS has already been observed by Chen et al.[12] in a study about the effect of the PDR on high-density neat and talc-filled polyethylene foamed at different saturation pressures. In particular, they observed that the PDR effect is larger when the activation energy for the bubble nucleation is higher, which is the case of the neat polymer.[12] The activation energy for nucleation will be defined in the modeling section.

In Figure 4, the effect of the PDR on ρ for talc-filled PS foams is shown at different T_{foam} values. As was already

DOI: 10.1021/acs.iecr.5b04911
Ind. Eng. Chem. Res. XXXX, XXX, XXX−XXX

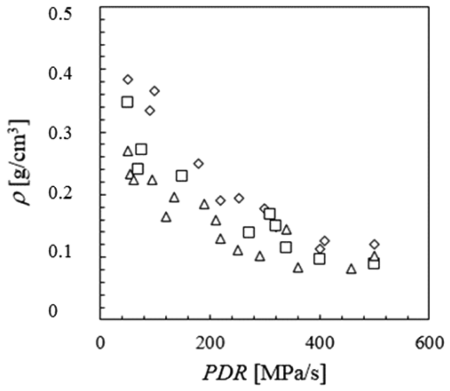

Figure 4. ρ of talc-filled PS as a function of the PDR and at different T_{foam} values (◇, 90 °C; □, 100 °C; △, 110 °C).

explained for the case of neat PS as a function of the PDR, a decrease of ρ with an increase of the PDR and with an increase of T_{foam} is observed for talc-filled PS foams. In this case, the minimum achievable ρ is 0.08 g/cm^3, ca. 30% bigger than the minimum ρ achieved with neat PS. This observation is in accordance with the fact that, under the investigated processing conditions, ρ decreases with T_{foam} because, in the testing conditions under investigation, the phenomenon governing the ρ decrease is bubble growth (larger for neat PS).[13] Possibly, furthermore, a delay in the achievement of a plateau value is observed (in this case, the minimum in the density is attained at ca. 400 MPa/s and higher).

In Figure 5, characteristic SEM images of samples at different T_{foam} and PDR values for neat and talc-filled PS foams are

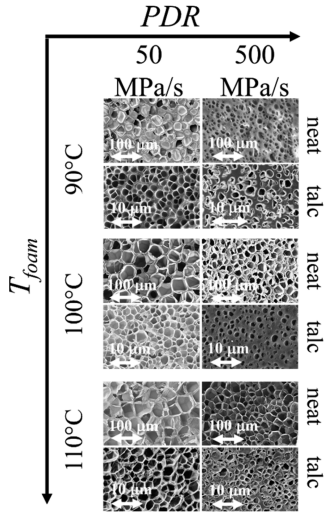

Figure 5. SEM images showing neat and talc-filled PS foam morphologies at different PDRs and T_{foam} values.

reported, evidencing what was already obtained with Figures 1−4. Note the need for using a larger magnification for the cases of talc-filled samples to properly show the foam morphology. The SEM images, reported in Figure 5, show uniform bubble morphology on the entire surface, and no bubble size gradient (e.g., induced by a temperature or a PDR nonuniformity) is observed at all of the PDRs investigated in the present work. As discussed before, in the minibatch, the dimensions of our samples and of the vessel are small enough not to induce any temperature and PDR local gradient.

MODELING

The foaming experiments and the results discussed in the previous paragraphs were used to model the effect of the PDR and T_{foam} on N, by recalling the considerations introduced by Muratani et al.[14] In the final part of this section, the gathered modeling tool is used and validated to design foams with target morphologies.

As was described earlier, N shows both PDR and T_{foam} dependence, with N increasing with the PDR and decreasing with T_{foam}. Speculating on the correlation between N and T_{foam}, it is possible, at any PDR value, to describe the aforementioned dependences by an exponential law,[2] as in eq 1:

$$\dot{n}(T_{foam}, \mathrm{PDR}) = \dot{n}(T_0, \mathrm{PDR}) \exp\left[\frac{E_{app}}{R}\left(\frac{1}{T_{foam}} - \frac{1}{T_0}\right)\right] \quad (1)$$

where $\dot{n}$, T_0, E_{app}, and R are respectively the bubble nucleation rate (i.e., number of nucleated bubbles per unit of time and initial volume), reference temperature, "apparent" activation energy,[17] and ideal gas constant.

The number of nucleated bubbles per unit of initial volume, N, can be estimated by multiplying $\dot{n}$ and the characteristic time of the process, given by P_{sat}/PDR. Hence, eq 1 now reads:

$$\dot{n}(T_{foam}, \mathrm{PDR})\frac{P_{sat}}{\mathrm{PDR}} = \dot{n}(T_0, \mathrm{PDR})\frac{P_{sat}}{\mathrm{PDR}}\exp\left[\frac{E_{app}}{R}\left(\frac{1}{T_{foam}} - \frac{1}{T_0}\right)\right] \quad (2)$$

Therefore

$$\ln\left[\frac{N(T_{foam}, \mathrm{PDR})}{N(T_0, \mathrm{PDR})}\right] = \frac{E_{app}}{R}\left(\frac{1}{T_{foam}} - \frac{1}{T_0}\right) \quad (3)$$

Using eq 3 to fit data at the different T_{foam} values, in the case of neat PS, considering 100 °C as T_0, and 100 MPa/s as the reference PDR, returns E_{app} = −165 kJ//mol. The time−temperature shift factor (a_T) can be estimated by the following equation:[14]

$$\ln a_T = \frac{E_{app}}{2.303R}\left(\frac{1}{T_{foam}} - \frac{1}{T_0}\right) \quad (4)$$

Figure 6 shows a_T at different T_{foam} values. It is evident that ln a_T linearly decreases with $1/T_{foam} - 1/T_0$.

As was explained,[14] the use of the shift factor allows one to shift data along the PDR axis at different T_{foam} values:

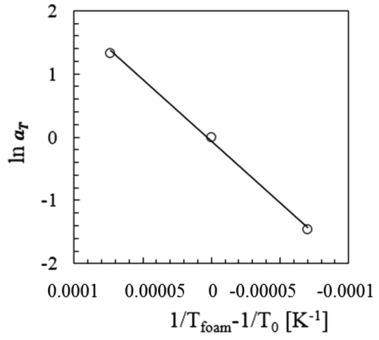

Figure 6. Effect of T_{foam} on a_T. The solid black line is obtained by interpolation with eq 4.

DOI: 10.1021/acs.iecr.5b04911
Ind. Eng. Chem. Res. XXXX, XXX, XXX−XXX

$$N(T_0, \mathrm{PDR}) = N(T_{foam}, \mathrm{PDR}a_T) \quad (5)$$

Figure 7 shows construction of the master curve. Figure 7a shows the relationship between N and the PDR at different

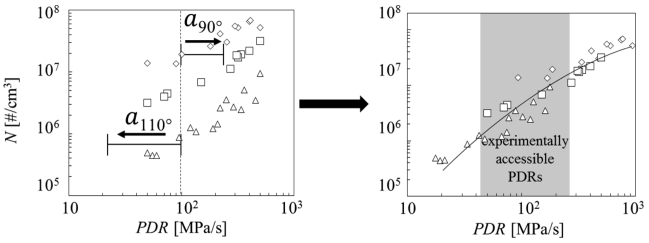

Figure 7. Procedure to build a master curve. (a) Raw experimental data of N versus PDR at different T_{foam} values (◇, 90 °C; □, 100 °C; △, 110 °C) and how the data at 110 and 90 °C were shifted. (b) Shifted data, with the experimentally accessible PDR range indicated with the gray window. The solid line is the master curve obtained as described in the text.

T_{foam} values, as was already discussed in Figure 1, and the values of a_T at 90 and 110 °C (100 °C has been used as a reference temperature). Figure 7b was obtained by shifting the experimental curves of N versus PDR for neat PS by a_TPDR. Hence, data at T_{foam} of 110 °C, with a_T lower than 1, were shifted toward the left, and data at T_{foam} of 90 °C, with a_T higher than 1, were shifted toward the right. The master curve for the neat PS foam at 100 °C is given by interpolation of the data at three different temperatures, as shown in Figure 7b. As is clear in Figure 7b, finally the shifted data based on T_{foam} equal to 100 °C make it possible to increase the range of experimentally accessible PDRs (i.e., gray window) from ca. 10 MPa/s up to ca. 1000 MPa/s.

Figure 7b shows variation of N on the entire extended range of the PDR and the fitting in terms of the solution of the best equation that has found describing the data in accordance with the behavior of b as a function of the PDR. Herein the slope of N as a function of the PDR at different T_{foam} and b values decreases linearly with the PDR in a logarithmic scale, and then a good fitting equation reads

$$N = c\mathrm{PDR}^{[-d\ \ln(\mathrm{PDR}/\mathrm{PDR}_0)+e]} \quad (6)$$

where c, d, and e are fitting parameters[22] and PDR_0 is the PDR at which N is equal to $c\mathrm{PDR}^e$. In particular, Table 1 reports the values for the neat and talc-filled PS samples.

Table 1. Fitting Parameters of Equation 6 for the Neat and Talc-Filled PS Samples

	c [s/(cm³·MPa)]	d	e
neat PS	1700	0.13	2.4
talc-filled PS	28000	0.10	1.6

It is worth noting that the slope of the master curve (i.e., eq 6) changes very slowly, and this justifies the fitting reported in Figures 1 and 3, where the slope of N versus PDR on the small range can be approximated as constant. Furthermore, for the sake of simplicity, we decided not to include the effect of the PDR on the shift factor.

In the same manner as was explained for construction of the master curve for neat PS, a master curve for talc-filled PS was built. In Figure 8, the talc-filled PS master curve (dashed line) is compared to the neat PS master curve. The result is that a

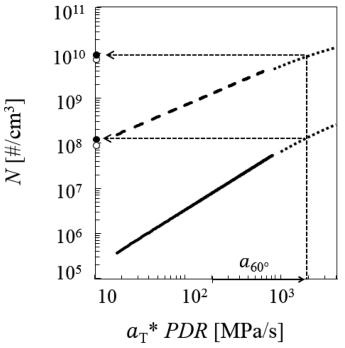

Figure 8. Master curves for neat (solid line) and talc-filled (dashed line) PS. An extrapolation of the curves (dotted lines) can be used to design the foaming process in a larger PDR range or at different T_{foam} values using accessible PDR. The open circles (○) represent the experimental N, while the closed symbols (●) are the model results.

lower apparent activation energy (−97 kJ/mol) was calculated for talc-filled PS with respect to neat PS.[19]

MORPHOLOGY-DESIGN TOOL

In order to verify any predicting capability of the present approach and to finally build a design tool to achieve the desired foam morphologies (target morphology, $\bar{N}$), we performed an experiment at T_{foam} = 60 °C and PDR = 190 MPa/s, which by scaling to the reference temperature of 100 °C means an extrapolated PDR = 1070 MPa/s (see Figure 8), quite far from the accessible experimental window reported in Figure 7b. PDR extrapolation has been performed based on eq 4, with a resulting a_{60} = 5.6. Figure 9 shows SEM images of neat

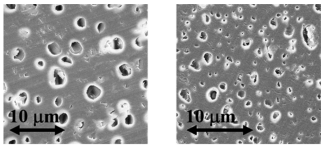

Figure 9. SEM images of (a) neat and (b) talc-filled PS foams, with P_{sat} = 10 MPa and T_{foam} = 60 °C.

and talc-filled PS foamed at T_{foam} of 60 °C and PDR = 190 MPa/s. The morphologies are finer than the ones foamed at higher temperature (see Figure 4), with smaller cell sizes and ρ = 0.8 g/cm³. In particular, for neat PS, $N = 9.3 \times 10^7$ #/cm³, while for talc-filled PS, $N = 8.4 \times 10^9$ #/cm³ (open symbols in Figure 8). To verify the approach, eq 5 can be used to calculate N at 60 °C and 190 MPa/s (corresponding to 100 °C and 1070 MPa/s), resulting in 1.5×10^8 #/cm³ and 9.5×10^9 #/cm³ for neat and talc-filled PS (closed symbols in Figure 8), respectively, which perfectly match the experimental data, proving the good predicting capability of the model at hand, as reported also in Figure 8. It is worth noting that said extrapolation should be performed with caution because phenomena like polymer vitrification at decreasing temperature may limit the extensibility of the model.

In conclusion, these results prove that once master curves have been experimentally validated, for the neat polymer or for any polymer-additive mixture, they can be used to design the

DOI: 10.1021/acs.iecr.5b04911
Ind. Eng. Chem. Res. XXXX, XXX, XXX−XXX

foaming process to achieve the desired $\bar{N}$. In effect, the horizontal line that intercepts $\bar{N}$ will cross the master curves, giving the $\overline{PDR}$ necessary to achieve $\bar{N}$. Now, if this $\overline{PDR}$ lies outside the experimentally accessible window, eq 5 will give the temperature shift factor needed to move horizontally in the experimentally accessible PDR window.

CONCLUSIONS

In this paper, some insight on bubble nucleation at high PDRs and at different T_{foam} values was gained. In particular, N was observed to be linearly increasing with PDR in a log−log scale at all of the investigated T_{foam} values (i.e., 90, 100, and 110 °C), even at very high PDRs. The effect of talc as the nucleating agent does not qualitatively change the effect of the PDR on N; however, it reduces the PDR influence on N, while at the same PDR, it induces a 3 orders of magnitude increase in N respect to neat PS. A phenomenological model to predict N at different PDR and T_{foam} values was presented and validated for the PS/CO_2 system. This easy approach provides a tool to achieve a target morphology by means of master curves describing the combined effect of both T_{foam} and PDR on N.

AUTHOR INFORMATION

Corresponding Author

*E-mail: edimaio@unina.it. Phone: +39 081 768 25 11. Fax: +39 081 768 24 04.

Notes

The authors declare no competing financial interest.

ACKNOWLEDGMENTS

Rete di Eccellenze Mastri (MAteriali e STRutture Intelligenti, POR Campania FSE 2007/2013, Codice 4-17-3) is acknowledged for partial support of this work.

ABBREVIATIONS

E_{app} = "apparent" activation energy
N = cell nucleation density
$\bar{N}$ = target cell nucleation density
$\dot{n}$ = bubble nucleation rate
PDR = pressure drop rate
$\overline{PDR}$ = target pressure drop rate
PS = polystyrene
PP = polypropylene
P_{sat} = saturation pressure
R = ideal gas constant
T_0 = reference temperature
T_{foam} = foaming temperature
T_{sat} = saturation temperature

REFERENCES

(1) Colton, J. S.; Suh, N. P. The nucleation of microcellular thermoplastic foam: Process model and experimental results. *Adv. Manuf. Processes* **1986**, *1*, 341.
(2) Colton, J. S.; Suh, N. P. The nucleation of microcellular thermoplastic foam with additives: Part I: Theoretical considerations. *Polym. Eng. Sci.* **1987**, *27*, 485.
(3) Park, C. B.; Behravesh, A. H.; Venter, R. D. Low density microcellular foam processing in extrusion using CO_2. *Polym. Eng. Sci.* **1998**, *38*, 1812.
(4) Guo, Q.; Wang, J.; Park, C. B.; Ohshima, M. A microcellular foaming simulation system with a high pressure drop rate. *Ind. Eng. Chem. Res.* **2006**, *45*, 6153.
(5) Taki, K. Experimental and numerical studies on the effects of pressure release rate on number density of bubbles and bubble growth in a polymeric foaming process. *Chem. Eng. Sci.* **2008**, *63*, 3643.
(6) Tsivintzelis, I.; Angelopoulou, A. G.; Panayiotou, C. Foaming of polymers with supercritical CO_2: an experimental and theoretical study. *Polymer* **2007**, *48*, 5928.
(7) Zeldovich, J. Theory of formation of a new phase cavitation. *J. Exp. Theor. Phys.* **1942**, *12*, 525.
(8) Khan, I., Costeux, S.; Adrian, D.; Bunker, S. Numerical studies of nucleation and bubble growth in thermoplastic foams at high nucleation rates. *FOAMS conference proceedings*; SPE: Seattle, WA, 2013.
(9) Tammaro, D.; Contaldi, V.; Carbone, M. P.; Di Maio, E.; Iannace, S. A novel lab scale batch foaming equipment the mini-batch. *J. Cell. Plast.* **2015**, DOI: 10.1177/0021955X15584654.
(10) Muratani, K.; Shimbo, M.; Miyano, Y. Correlation of decompression time and foaming temperature on the cell density of foamed polystyrene. *Cell. Polym.* **2005**, *24*, 198.
(11) Sato, Y.; Takikawa, T.; Takishima, S.; Masuoka, H. Solubilities and diffusion coefficients of carbon dioxide in poly(vinyl acetate) and polystyrene. *J. Supercrit. Fluids* **2001**, *19*, 187.
(12) Chen, L.; Sheth, H.; Wang, X. Effects of shear stress and pressure drop rate on microcellular foaming process. *J. Cell. Plast.* **2001**, *37*, 353.
(13) Arora, K. A.; Lesser, A. J.; Mccarthy, T. J. Preparation and characterization of microcellular polystyrene foams processed in supercritical carbon dioxide. *Macromolecules* **1998**, *31*, 4614.
(14) Muratani, K.; Shimbo, M.; Miyano, Y. Correlation of decompression time and foaming temperature on the cell density of foamed polystyrene. *Cell. Polym.* **2005**, *24*, 271.
(15) Lee, M.; Park, C. B.; Tzoganakis, C. Measurements and modeling of PS/Supercritical CO_2, solution viscosities. *Polym. Eng. Sci.* **1999**, *39*, 99.
(16) Lee, P. C.; Li, G.; Lee, J. W. S.; Park, C. B. Improvement of cell opening by maintaining a high temperature difference in the surface and core of a foam extrudate. *J. Cell. Plast.* **2007**, *43*, 431.
(17) Alvarez-Idaboy, J. R.; Mora-Diez, N.; Vivier-Bunge, A. A quantum chemical and classical transition state theory explanation of negative activation energies in OH addition to substituted ethenes. *J. Am. Chem. Soc.* **2000**, *122*, 3715.
(18) Knauer, O. S.; Pastore Carbone, M. G.; Braener, A.; Di Maio, E.; Leipertz, A. Investigation of CO_2 in molten polymers at high pressures using Raman line imaging. *Polymer* **2013**, *54*, 812.
(19) Wang, C.; Leung, S. N.; Bussmann, M.; Zhai, W. T.; Park, C. B. Numerical investigation of nucleating-agent-enhanced heterogeneous nucleation. *Ind. Eng. Chem. Res.* **2010**, *49*, 12783.
(20) Wong, A.; Park, C. B. The effects of extensional stresses on the foamability of polystyrene−talc composites blown with carbon dioxide. *Chem. Eng. Sci.* **2012**, *75*, 49.
(21) Marrazzo, C.; Di Maio, E.; Iannace, S. Conventional and nanometric nucleating agents in poly (ε -caprolactone) foaming: crystals vs bubbles nucleation. *Polym. Eng. Sci.* **2008**, *48*, 336.
(22) Nelder, J. A. The fitting of a generalization of the logistic curve. *Biometrics* **1961**, *17*, 89.
(23) Khan, I.; Adrian, D.; Costeux, S. A model to predict the cell density and cell size distribution in nano-cellular foams. *Chem. Eng. Sci.* **2015**, *138*, 634.
(24) Costeux, S.; Khan, I.; Bunker, S. P.; Jeon, H. K. Experimental study and modeling of nanofoams formation from single phase acrylic copolymers. *J. Cell. Plast.* **2015**, *51*, 197.
(25) Leung, S. N.; Wong, A.; Park, C. B.; Guo, Q. Strategies to estimate the pressure drop threshold of nucleation for polystyrene foam with carbon dioxide. *Ind. Eng. Chem. Res.* **2009**, *48*, 1921.
(26) Pastore Carbone, M. G.; Di Maio, E.; Scherillo, G.; Mensitieri, G.; Iannace, S. Solubility, mutual diffusivity, specific volume and interfacial tension of molten PCL/CO_2 solutions by a fully experimental procedure: effect of pressure and temperature. *J. Supercrit. Fluids* **2012**, *67*, 131.

DOI: 10.1021/acs.iecr.5b04911
Ind. Eng. Chem. Res. XXXX, XXX, XXX−XXX